

Quaternary glacial chronology of the Ateoyinake River Valley, Tianshan Mountains, China

Jingdong Zhao^{a,b,*}, Shiyin Liu^a, Yuanqing He^a, Yougui Song^c

^a State Key laboratory of Cryospheric Science, Cold and Arid Regions Environmental and Engineering Research Institute, Chinese Academy of Sciences, Lanzhou, 730000 China

^b Institute of Tibetan Plateau Research, Chinese Academy of Sciences, Beijing, 100085 China

^c Institute of Earth Environment, Chinese Academy of Sciences, Xi'an, 710075 China

ARTICLE INFO

Article history:

Received 1 April 2007

Accepted 20 December 2007

Available online 8 May 2008

Keywords:

ESR dating

Marine oxygen isotope stages (MIS)

Tianshan Mountains

Glacial chronology

Central Asia

ABSTRACT

The Ateoyinake River originates on the southern slope of the Tumor Peak, the largest center of modern glaciation in the central Tianshan Mountains in China. Six sets of moraines and associated glacial sediments are well-preserved in the Ateoyinake River drainage, recording a complex history of Quaternary glacial cycles and landscape evolution. Dating the landforms allow the temporal and spatial shifts of past cryosphere and climate to be determined. Dating of the tills and outwashes was undertaken with electron spin resonance (ESR) and optically stimulated luminescence (OSL). Two OSL ages date outwash and till to 7.3 ± 0.8 ka and 12.3 ± 1.2 ka, respectively. The ESR ages date six sets of moraines to 3.4 ka, 14–27 ka, 40–54 ka, 55–62 ka, 134.4 ± 12.6 ka and 219.7 ± 20.5 ka, 440.6 ± 41.7 ka. If these are correct ages of deposition, they suggest that glaciers advanced during the Neoglacial and during marine oxygen isotope stages (MIS) 2, 3b, 4, 6 and 12. The MIS 3b moraine was created by a glacier nearly as large as or possibly larger than those of the “global” Last Glacial Maximum of MIS 2. The oldest till belongs to the “Qingshantou Glacial Stage”. Its single age is consistent with two published ESR ages (459.7 ± 46 and 471.1 ka) from the Gaowangfeng till near the headwaters of the Ürümqi River in the eastern Tianshan Mountains. These dates suggest that the central and the eastern segments of the Tianshan Mountains were high enough to be glaciated by MIS 12. The geochronology of the glacial landforms in this valley is the first step towards understanding glacial and landscape evolution in this region. Furthermore, this geochronology and previously published geochronology near the headwaters of the Ürümqi River provide a temporal framework for examining the rates of landscape evolution in the glaciated regions of the Tianshan Mountains.

Crown Copyright © 2008 Published by Elsevier B.V. All rights reserved.

1. Introduction

Mountain glaciers are important geomorphic agents in shaping the landscapes of glaciated regions, and are responsible for carving some of the most spectacular landscapes on Earth. The landscape contains considerable information on past glacial processes in the form of moraines and other depositional landforms. In alpine areas, glaciers are widely accepted as having sustained high rates of erosion, and generally large glaciers can erode more rapidly than smaller ones, particularly in the ablation zone (Hallet et al., 1996; Brocklehurst and Whipple, 2006). In active tectonic settings, glacier-driven erosion has the potential to influence climate by increasing chemical weathering and, ultimately, lowering atmospheric concentrations of CO₂ (Raymo and Ruddiman, 1992). In addition, glaciers enhanced rates of valley incision during glaciation and isostatic rebound would cause the high crests to rise, especially, in some alpine area, where the mountain

ranges have high crests and deep valleys. The changes in relief have been suggested to influence the climate through the uplift of mountain crests (Molnar and England, 1990). The characteristic glacial landforms and bedrock topography are also studied to deduce the former properties of the glaciers, and lead to a good understanding of the temporal and spatial shifts of the past glaciers.

Glaciers are highly sensitive to climate change and in China are known as “the thermometer of the landmass” (Shi et al., 2000). A glacier responses to climate directly influences geomorphic processes, sediment transfer and landscape evolution. As a consequence, abundant Quaternary glacial landforms and sediments are well-preserved in many regions throughout China. Dating glacial landforms is a fundamental requirement in studying the landscape evolution of the past cryosphere. During the past several decades, dating techniques, including cosmogenic radionuclide (CRN: e.g., Finkel et al., 2003; Owen et al., 2006a,b), electron spin resonance (ESR: e.g., Zhou et al., 2002a,b; Yi et al., 2002; Zhao et al., 2006), thermoluminescence (TL: e.g., Zhang et al., 2005) and optically stimulated luminescence (OSL: e.g., Spencer and Owen, 2004), can potentially directly determine ages of the glacial sediment and landforms. These techniques have been refined and applied widely.

* Corresponding author. State Key laboratory of Cryospheric Science, Cold and Arid Regions Environmental and Engineering Research Institute, Chinese Academy of Sciences, Lanzhou, 730000 China.

E-mail address: jdzhao@lzb.ac.cn (J. Zhao).

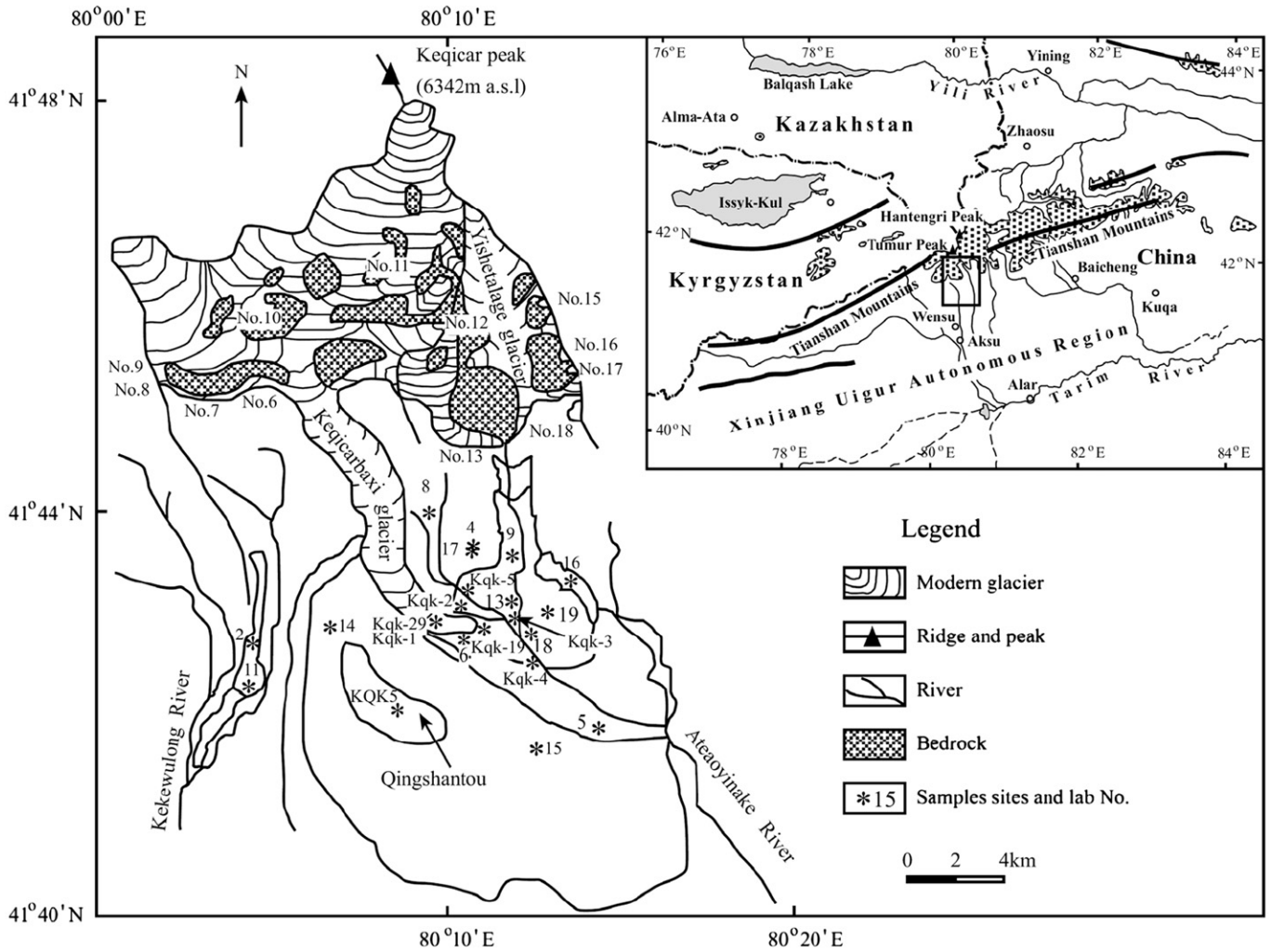


Fig. 1. Modern glaciers and sampling sites in the Ateayinake River.

Research on Quaternary glaciations has entered a new stage in which the emphasis is on accurate dating, with quantitative techniques augmenting conventional mapping and relative dating.

Reviewing the literature, Gillespie and Molnar (1995) suggested that maximum advances of glaciers were not synchronous globally. Since then, many studies have tested and partially confirmed this view. In particular, large-scale glacier advances in High Asia appear to have occurred in marine oxygen isotope stage (MIS) 3 or earlier, with the extent of the glaciers exceeding that during the global Last Glacial Maximum (LGM_C) (e.g., Owen et al., 2002a,b,c, 2003, 2006a,b; Zech et al., 2003; Kamp et al., 2004). In China, Shi and Yao (2002) divided MIS 3 into three sub-stages (a, b and c) on the basis of the isotopic record and climatic characteristics inferred from the Guliya ice core. They concluded that MIS 3b (44–54 ka) was cold and wet. Furthermore, they concluded from published studies that a large glacier advance occurred during MIS 3b, which has been identified in 23 sites in twelve regions throughout Asia, Europe, Oceania, North and South America.

This study focuses on the Tianshan Mountains, a large mountain system in Central Asia. These mountains are tectonically active and stretch ~2500 km, and are ~1700 km long along latitude ~43°N in the Xinjiang Uigur Autonomous Region, China. They comprise many sub-parallel, East–West trending mountain ranges and valleys, with the highest peak being Tumor Peak (7435.3 m asl), which is the center of modern glaciation in the Tianshan Mountains. Quaternary glaciations of this region have been studied since the 1940 s (e.g., Huang, 1944; Feidaoluweiqi and Yan, 1959, 1960; Liu et al., 1962; Geography

department of Nanjing University, 1974; Shi et al., 1984; Su et al., 1985; Zheng, 1985). Contentions exist, however, over the number and timing of glaciations in this region because researchers have not been able to define the timing of glaciation. Refining the glacial chronology is a first step towards understanding the landscape evolution and paleoclimate

Table 1
Dimensions of the modern glaciers in the Ateayinake River basin

Glacier number or name	Length (km)	Top (m asl)	Median (m asl)	Terminus (m asl)	Area (km ²)	Ice volume (km ³)
Keqicarbaxi glacier	26	6040	4460	3060	83.56	15.7928
No. 6	0.3	4734	4680	4600	0.07	0.0007
No. 7	0.2	4728	4620	4540	0.19	0.0030
No. 8	0.5	4880	4600	4500	0.14	0.0020
No. 9	0.3	4840	4680	4600	0.21	0.0036
No. 10	0.8	5147	4740	4400	0.75	0.0225
No. 11	0.3	5253	5000	4800	0.22	0.0037
No. 12	0.2	5055	4980	4900	0.12	0.0016
No. 13	6.1	5256	4160	3460	6.24	0.5054
Yishetalage glacier	8.2	5478	4300	3432	14.77	1.5952
No. 15	0.3	4960	4880	4700	0.09	0.0011
No. 16	0.2	4600	4500	4440	0.09	0.0011
No. 17	0.3	4600	4500	4420	0.16	0.0024
No. 18	0.3	4660	4520	4280	0.15	0.0023

Locations are shown on Fig. 1.

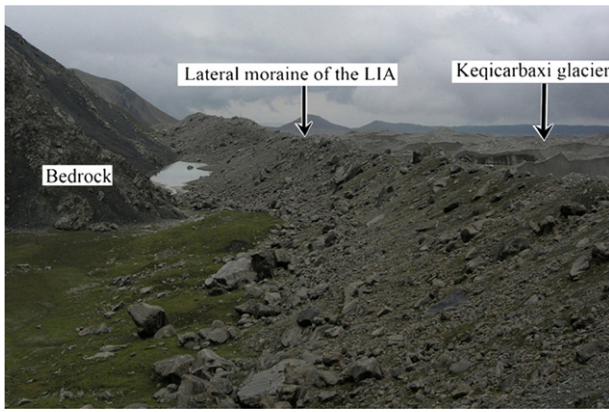


Fig. 2. Lateral moraine of the LIA on the north side of the Keqicarbaxi glacier (~3650–3600 m asl).

in this part of Central Asia. Recently, we have used the ESR and OSL dating methods in an attempt to determine the timing of glacial landforms in the Ateaoyinake River Valley, which is on the southern slopes of Tumor Peak. This paper will, therefore, describe the Quaternary glacial deposits and landscapes, and present new ESR and OSL ages for the timing of glaciation in this valley.

2. The Ateaoyinake River Valley

The Ateaoyinake River (41°48′–41°35′N, 80°03′–80°27′E) originates from the southern slopes of Tumor Peak and flows southwards into the Tarim Basin. The river has an annual discharge of $\sim 1.1 \times 10^8 \text{ m}^3$, with >80% being glacier meltwater. The water provides a vital resource for the oases in the northern part of Wensu County.

The mountain ridges above the drainage are between 4000 and 5300 m asl, and the highest peak is Keqicar (6342 m asl). Fourteen modern glaciers exist in headwaters of the Ateaoyinake River with the

modern equilibrium-line altitude (ELA) at $\sim 4500 \text{ m asl}$ (Fig. 1). These include compound and simple valley glaciers, cirque glaciers and hanging glaciers (Table 1), with a total area is about 107 km^2 and an ice volume is about 18 km^3 (Lanzhou Institute of Glaciology and Geocryology, CAS, 1985). The Keqicarbaxi glacier, the largest compound valley glacier, has its terminus is at 3060 m asl, and stretches for >1400 m below the ELA ($\sim 4500 \text{ m asl}$). The glacier is covered by supraglacial till that is 2–3.5 m thick, but becomes thinner with the height until above 3960 m asl, where the glacier surface is debris free.

The climate of this area is dominated by mid-latitude westerlies, with precipitation directly influenced by westerly circulation. Meteorological data (e.g., temperature, precipitation) have been observed and obtained by our research group. Records from September 2004 to August 2005 of the artificial observation station (3009 m asl), show the annual precipitation is 669.4 mm at 3009 m asl. Most of the precipitation falls in summer months, $\sim 81\%$ between May and October and $\sim 55\%$ between June and August. The annual precipitation at two other rain gauges at ~ 3700 and $\sim 4200 \text{ m asl}$ are 566 mm and 830 mm, respectively. These records show that the precipitation decreases first and then increases with altitude. Precipitation near the ELA is $\sim 1000 \text{ mm}$. Based on the records from 2003 to 2006 of the artificial observation station and two automatic weather stations operating on the glacier at ~ 3700 and $\sim 4200 \text{ m asl}$, the mean annual temperatures are $0.5 \text{ }^\circ\text{C}$, $-3.75 \text{ }^\circ\text{C}$ and $-6.56 \text{ }^\circ\text{C}$, respectively. These data indicate that the temperature in the region is strongly controlled by altitude, with an environmental lapse rate of $\sim 0.6 \text{ }^\circ\text{C}/100 \text{ m}$. The mean annual temperature at ELA is $\sim -8.36 \text{ }^\circ\text{C}$.

3. Quaternary glacial sediments

3.1. Modern and Little Ice Age moraines

Glaciers during the Little Ice Age (LIA) advanced $\sim 300\text{--}500 \text{ m}$ beyond the present cirques and hanging glaciers, and commonly formed one to three end moraines. The valley glaciers also advanced

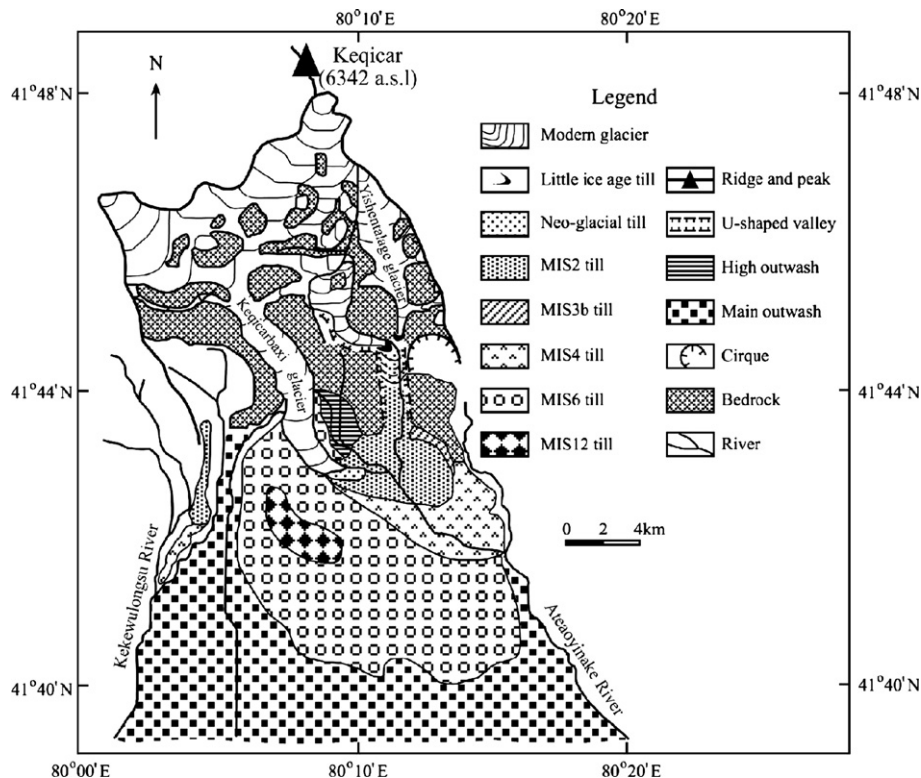


Fig. 3. Map of glacial landforms in the Ateaoyinake River.

during the LIA, but these moraines are poorly preserved. The LIA moraines show little evidence for erosion and boulders on the moraines are unweathered and commonly striated. The till comprises granite, gneiss, sandstone, conglomerate, limestone and shale clasts. Soil is absent, and the only vegetation on the boulders includes pioneering plants such as lichen, moss.

Moraines occur on either side of the Keqicarbaxi glacier rising 5–20 m above the ice (Fig. 2). Striated boulders on the inner crests are fresh and unweathered, but those on the outer crest have incipient weathering. The inner crest is devoid of vegetation, but the outer crests support pioneering plants, and even some shrubs grow in sheltered locations at lower elevations. Dendrochronology on shrubs collected at about 3100 m asl provides a minimum age of 72–77 years, supporting the view that the moraines formed during the LIA.

3.2. The U-shaped valley to the piedmont

Six sets of moraines are present from the snout of the Keqicarbaxi glacier to the piedmont (Figs. 3 and 4), extending 11 km to an altitude of about 2100 m asl. The youngest set of moraines is present at two sites, one at the terminal of the Keqicarbaxi glacier and the other in the well-developed U-shaped valley that contains the No. 13 and Yishentalage glaciers. The U-shaped valley is ~5 km long. Several end moraines, about 0.2 to 1 km wide and 3 to 10 m high, are present within 1 km of the modern Keqicarbaxi glacier. These extend down to 2990 m asl. Parts of these end moraines were overrun by the glacier during the 1940s to 1970s (Su et al., 1985). Since then the glaciers have been in retreat. A layer of fresh till marks to locations where the moraines were overrun. The till comprises granite, gneiss, sandstone, conglomerate and red mudstone clasts.

Three end moraines are present in the U-shaped valley and extend ~1 km. The inner-most end moraine is ~1.2 km from the snout of the Yishentalage glacier, and is ~60 m wide and 3–6 m high. The middle end moraine is ~150 m wide and 5–8 m high. The outermost end moraine, the largest of the three, is ~400 m wide and 6–10 m high. All three moraines have a 20 cm-thick gray soil. The tills consist of granite, schist, limestone and gneiss clasts.

The second set of moraines occurs within 1–5 km of the snout of the Keqicarbaxi glacier and within 5 km of the Yishentalage glacier, at an altitude of between 2990 to 2700 m asl. The total area is about 12 km². This set includes several large end moraines that are overlain by a 70–80 cm-thick deposit of loess. A 20–30 cm thick gray-cinnamon

soil is developed in the loess. The surface of some boulders are weathered. The till clasts consist of granite, schist, gneiss, shale, and limestone. The location of the second set of moraines shows that the Keqicarbaxi glacier, the Yishentalage glacier, and the No. 13 glacier once coalesced to form a large compound valley glacier.

The third set of moraines is ~13 km², only slightly larger than that of the second set, which overlies them. The tills consist of granite, gneiss, shale, red mudstone and red sandstone clasts. The morphostratigraphic relationships and lithologies suggest that the tills were deposited during different glaciations. End moraines from the third set occur northeast of the second set of moraines. The area of the exposed moraines is 1 km² and they are ~200–350 m wide and 30–50 m high.

The fourth set of moraines occurs between 2700 to 2250 m asl and has an area of 20 km². Several end moraines with arcs in the southeast occur between 2500 m to 2250 m asl and are 40–60 m high. These are overlain by 1.3 m-thick deposits of loess in which a 30 cm-thick gray-cinnamon soil has developed. These moraines support sparse shrubs at the lower elevations. Till clasts below 2500 m asl consist of granite, quartzite, conglomerate, sandstone, schist, and shale.

The till of the fifth set of moraines is present on both sides of the Keqicarbaxi glacier (Fig. 5). This set of moraines is the largest in the succession, with an area 40 km² and a height of 3–20 m. Till is present from 3300 m down to 2100 m asl on the south side of the glacier. From the air the moraines look like a fan spreading from the north to the south on the pediment (Fig. 4). To the north, only a 3 km long and 200–500 m wide lateral moraine is present, and extends from 3250 m to 3040 m asl (Fig. 6). The till is compacted and well-cemented with silica and calcium carbonate. The exposed erratics are severely weathered, and the surfaces can be peeled off easily. The till has been buried by ~2 m of loess, a ~40 mm-thick soil which contained 4–6 charcoal debris layers has been developed in the loess, maybe, the charcoal debris layers indicated that several shrub fire have occurred here. Grasses grow well at higher altitudes on this till, but are thinner at lower altitudes. Sparse shrubs and scattered willows and aspens are present at lower elevations.

A high glaciated plateau is situated on the red Tertiary bedrock at about 3300 m asl on the south side of the Keqicarbaxi glacier (Fig. 4). The plateau is called “Qingshantou”, and its highest point is 3356 m asl. Moraines here are about 4–10 m high. Deeply weathered granite, gneiss and conglomerate boulders, 1–3 m in diameter (the largest being 8×6×2.5 m³) are present on the surface of the plateau. These

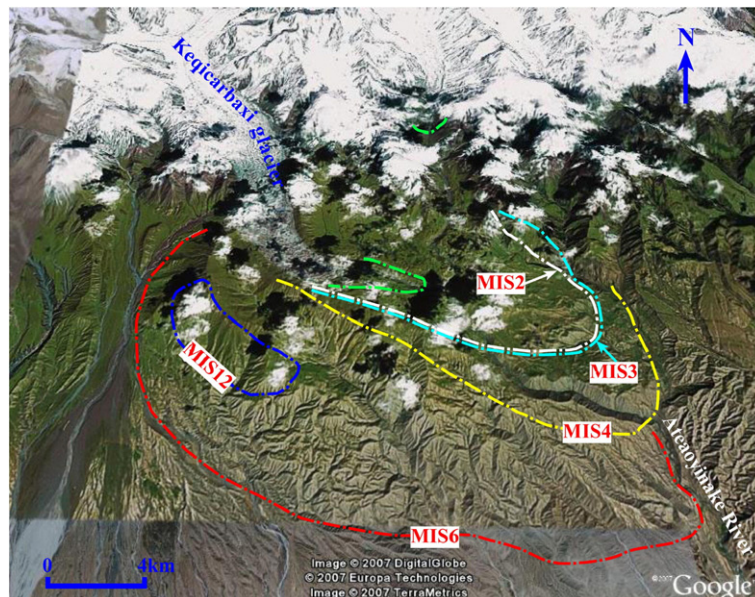


Fig. 4. Glacial sediment sequences in the Ateoyinake River.



Fig. 5. Lateral moraines on either side of the Keqicarbaxi glacier.

tills are well-cemented with silica. Till clasts include granite, gneiss, conglomerate and red sandstone.

The higher topographic position of the plateau and the greater degree of the weathering indicate that the tills are very old. We consider them to represent another glaciation, which we call the “Qingshantou glacial stage”. After this glaciation, the landforms underwent much erosion and the landscape during this glaciation would have been quite different from the present style. We speculate that the Qingshantou moraines were produced by an ice cap.

The Kekewulongsu River, ~3 km west to the Qingshantou glacial plateau, has two sets of moraines preserved on the east side. The first set is well-preserved, while the second set is not and is characterized by only scattered boulders on its surface. The first set is also overlain by a ~80 cm-thick deposit of loess, and ~25 cm-thick gray-cinnamon soil has developed. The property of weathering and compaction of this first set are similar to that of the second set in the Ateoyinake River valley. We suggest, therefore, that they formed during the same glaciation.

4. Methods

Samples for luminescence and ESR dating were collected from natural or artificial profiles, following the procedures in the fieldwork guides, which were processed by the ESR and OSL chronology laboratories. The samples were stored in opaque bags or boxes to ensure that they were not exposed to light or heated during transportation to the OSL chronology laboratory at the Cold and Arid Regions Environmental and Engineering Research Institute, Chinese Academy of Sciences (CAREERI, CAS), Lanzhou. Most samples were analyzed with the ESR dating technique and supplemented with OSL dating.

Each ESR sample was divided into two. One part was used to measure the water content and then was ground and sieved through a <0.1-mm screen. The crushed samples were used to determine the concentrations of radioactive elements (e.g. U, Th) and the contents of K₂O. The other part was washed and sieved to collect the 125–250 μm particle size fraction, which was treated with H₂O₂ to remove the organic materials. The sediment was placed in 6 mol/l HCl to remove carbonates. The quartz-rich fraction was prepared by heavy liquid separation. Then, the samples were treated with HF for 1 h to etch the surface of the grains which are commonly damaged by alpha rays. This procedure also helped to concentrate the quartz grains by dissolving non-quartz particles. Magnetic minerals were removed using a magnetic separator with a 2-A current.

The pretreated samples were divided into nine aliquots (about 250 mg each) and irradiated with different doses using ⁶⁰Co source. The doses were monitored with alanine/ESR dosimeters; the ratio was 15–45 Gy/m. The irradiated samples were stored untouched for >3 months. Ge centers were chosen as dating signals and measured with an ECS106ESR spectrometer manufactured by Bruker (Germany) in the Open Laboratory of Marine Sedimentology, Qingdao. The measurement conditions were as follows: room temperature; X-band; microwave power=2 mW; modulation amplitude=0.1 mT; central magnetic field=348 mT; sweep width=5 mT; change time:=5.12 mS; time constant=40.96 mS; and amplification=1 × 10⁵. The typical ESR spectra of the quartz samples are shown in Fig. 7.

Least-squares analysis was used to fit the data points on the basis of different artificial irradiation doses. The corresponding signal intensities and linear fits were chosen. The curve was then extrapolated to zero to obtain the total dose (TD) (Fig. 8).

The concentrations of U and Th and the contents of K₂O were determined by laser fluorescence, colorimetric spectrophotometry and atomic absorption, respectively. The cosmic ray contributions to dose rates was estimated and calculated following the formulas of Prescott and Hutton (1994). The annual dose rate (*D*) was estimated from the radioisotope concentrations and the cosmic ray contributions. Ages were obtained from:

$$\text{Age} = \frac{\text{TD}}{D}$$

where TD is the total dose, and *D* is the annual dose rate.

The two OSL samples were prepared under laboratory safelight conditions to avoid sample bleaching. The water content was determined by drying sub-samples. The sample for dating was dry-sieved to collect the 63 to 180 μm particle size fraction. The carbonates and organic matter were removed using HCl and H₂O₂, respectively. The quartz-rich fraction was prepared from the chosen particle size fraction by heavy liquid separation. Then, the separated quartz-rich fraction was treated with 40% HF for 1 h to dissolve any plagioclase feldspars and remove the alpha-irradiated surface of the quartz grains. Dried quartz grains were mounted on stainless steel discs using silicon spray. The prepared quartz grains were measured in a Riso DA-15 OSL/TL reader to determine equivalent dose (*De*) by the single aliquot regenerative (SAR) protocol of Murray and Wintle (2000). U, Th concentrations, and K₂O contents were determined directly by means of Neutron Activation Analysis (NAA) to an uncertainty of between 5%–10%. The environmental dose-rate (*D*)

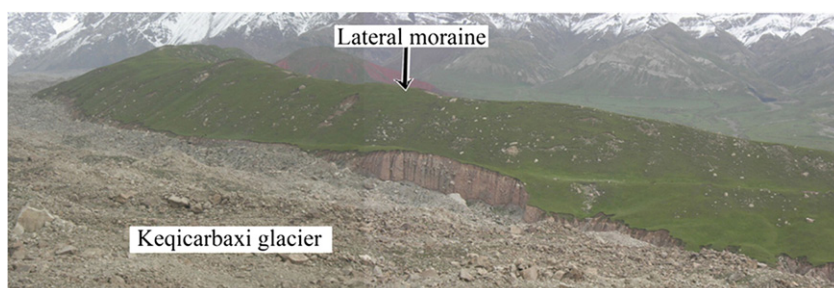


Fig. 6. Lateral moraine of MIS 6 on the north side of the Keqicarbaxi glacier (~3250–3040 m asl).

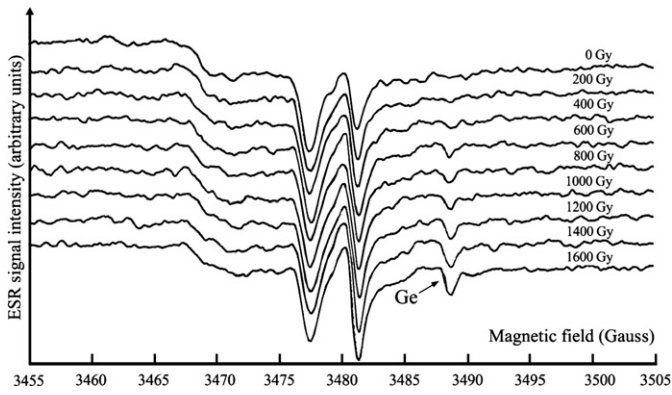


Fig. 7. Typical ESR spectra at room temperature (Sample No. 2).

was calculated using the concentrations of radioactive elements and the K_2O contents and cosmic dose rate using the formulas of Prescott and Hutton (1994). All measured results were converted to alpha, beta and gamma dose rates using the conversion factors of Adamiec and Aitken (1998). The water content reduces the dose rate and we estimate the uncertainty to be $\pm 5\%$.

5. Results

The ESR ages in stratigraphic order are consistent with the geological setting, weathering and cementation of the moraines. The ages correlate to the cold time in the marine oxygen isotope stage curve. In addition, the OSL age of 7.3 ± 0.8 ka for Kqk-29# and ESR age of 6.8 ± 0.6 ka for Kqk-1 provide a check on the reliability of the dating. The details of the sampling sites, the results of the dating, and correlated parameters are listed in Table 2.

6. Discussion

6.1. Mechanism of Ge centers bleaching in glacial quartz grains

The central assumption of the ESR dating technique is that the paramagnetic centers in quartz grains are bleached when they are heated, stressed/grinding, exposed to the sunlight or re-crystallized. After deposition, the paramagnetic centers are formed again by radiation emitted from natural radioactive elements and cosmic rays,

and then they become changed over time. Previous studies have shown that Ge centers in quartz grains are sensitive to sunlight or grinding, and that these mechanisms effectively could bleach the sediment (Tanaka et al., 1985; Buhay et al., 1988; Ye et al., 1993, 1998; Walther and Zilles, 1994). Tanaka et al. (1985) suggested that a 3 mm thin layer of the deltaic sands, the ESR signal at g-value of 1.997 (thought to be associated with the Ge center) disappeared completely after only seven hours of bleaching by sunlight. Therefore, they chose this center to date deltaic and beach sands and obtained dating results that they considered reasonable estimates of the true age. Subsequently, optical bleaching studies on the Ge centers by Buhay et al. (1988) on quartz grains from fault gouge and by Ye et al. (1993) on beach quartz sands, confirmed that Ge centers can be bleached within a few hours when exposed to an ultra-violet lamp or sunlight. Walther and Zilles (1994) observed that sunlight bleached the Ge signal to zero in about 2 days. Ye et al. (1998) conducted grinding experiments, and found that the intensity of the Ge centers decreased by 38% after the samples were ground for 1 min. They attributed the resetting of the Ge centers in quartz grains within debris-flow deposits to collisions between particles. Similarly, sediments within glaciers could also be reset by collisions between grains. In addition, the high silt content in glacial deposits and the microscopic studies of till quartz grains revealed that abrasion and crushing is very prevalent (Mahaney et al., 1988; Yi, 1997). Exposing or grinding sediment seems a reasonable mechanism to bleach the ESR signal. The OSL signals are also very sensitive to the light, and the sunlight easily bleaches sediments when glacial sediment is exposed to sunlight.

6.2. Glacial sediment sequences and a possible MIS3b glacier advance

The analysis of the glacial landforms and dating results show a complex and long history of landscape evolution in this valley (Figs. 3–5). Many researchers have suggested that the oxygen isotope record in marine sediment can be used as a proxy for climate and ice volumes on the land (Zhou and Li, 1998; Zhou et al., 2002a,b, 2006; Zhao et al., 2006). In addition, Shi and Yao's (2002) work on the Guliya ice core can be used to infer climate conditions for Central Asia.

The dating helps provide a temporal framework for examining the rates of landscape evolution. The ESR dating suggests that fresh-looking till within the first set of moraines formed at 3.4 ± 0.4 ka (Kqk-2). Although only a single ESR date was obtained, this age, if correct, suggests that glaciers in this valley advanced during Neoglacial. The Keqicarbaxi glacier was ~27 km long during this time. In addition,

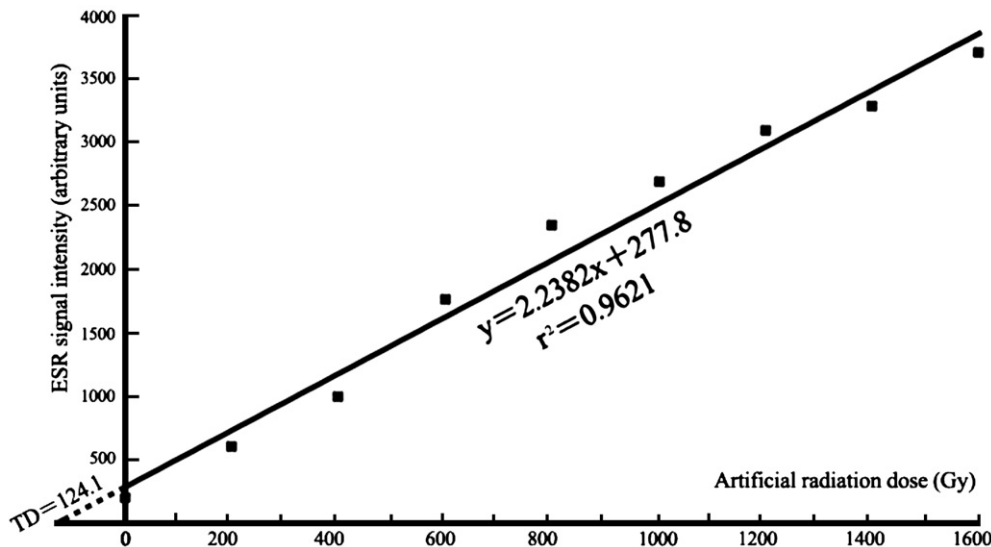


Fig. 8. An example of the best-fit line between artificial radiation doses and ESR signal intensity (Sample No. 2).

Table 2
ESR and OSL dating sampling sites and results (locations are shown on Fig. 1)

Lab no.	Samples' locations and description				U (ppm)	Th (ppm)	K ₂ O (%)	Cosmic* (mGy*a ⁻¹)	Water (%)	TD (Gy)	Age (ka)
	Location (N, E)	Asl (m)	Depth (m)	Samples' description							
Kqk-1	41°41'47"	80°09'34"	3034	19	1.72	23.1	3.6	0.0432	2.53	36.91	6.8±0.6
Kqk-2	41°41'50"	80°10'11"	3002	4.6	1.45	18.4	3.87	0.1818	7.81	17.55	3.4±0.4
Kqk-29 [#]	41°41'47"	80°09'34"	3034	19	1.87	4.87	2.42	0.0432	2	24.98±2.66	7.3±0.8
Kqk-19 [#]	41°41'37"	80°09'49"	3107	4.8	2.09	15	2.86	0.1807	3	52.26±5.07	12.3±1.2
6	41°41'31"	80°09'37"	3123	3.7	1.26	18.4	3.96	0.2111	9.67	72.3	14.3±1.3
9	41°43'33"	80°11'29"	3157	21	1.98	10.8	2.78	0.0406	4.31	67.7	18.1±1.8
											(at the exit of the Yishentalage River)
Kqk-5	41°42'08"	80°11'10"	3018	2.8	1.94	9.37	3.03	0.2353	5.06	69.53	17.4±1.6
Kqk-3	41°41'30"	80°12'01"	3006	15	1.68	23.6	3.19	0.0585	2.71	107.17	21.1±2.1
19	41°41'50"	80°12'40"	3058	11	1.87	14.6	3.08	0.0854	3.47	115.9	26.7±2.5
2	41°41'38"	80°03'41"	2816	1.2	2.17	29.1	3.44	0.2874	3.14	124.1	20.5±1.9
11	41°41'14"	80°04'13"	2835	1.3	1.21	5.5	3.58	0.2841	1.37	112.4	26.8±2.5
Kqk-4	41°41'13"	80°12'18"	2983	25	1.7	20.2	3.68	0.0330	4.03	210.91	40.9±4.0
											(derived from the bottom of the stream cut)
18	41°41'28"	80°12'16"	3021	28	1.54	16.4	3.46	0.0315	7.12	207.5	46.2±4.2
											(derived from the bottom of the stream cut)
13	41°41'58"	80°11'37"	2995	26	1.13	9.39	3.87	0.0323	1.73	227.5	51.0±4.8
											(derived from the bottom of the stream cut)
16	41°42'44"	80°13'13"	3117	31	1.94	11.7	3.5	0.0313	1.03	246.1	54.0±5.2
8	41°44'32"	80°08'55"	3054	15	1.16	23.4	3.67	0.0575	11.15	271.2	55.4±5.2
4	41°43'35"	80°11'41"	3071	1.8	2.41	13.3	2.87	0.2743	5.01	260.2	60.2±5.7
5	41°39'31"	80°14'13"	2928	17	1.2	14.8	0.016	0.0481	7.52	89.5	62.3±5.8
17	41°43'35"	80°11'41"	3072	2.9	3.4	10.6	2.7	0.2309	2.19	525.4	122.3±11.7
14	41°41'52"	80°06'09"	2850	1.8	1.16	3.99	1.14	0.2615	1.04	253.9	134.4±12.6
15	41°38'49"	80°12'42"	3109	2.1	1.42	12.7	2.94	0.2629	5.88	887.6	219.7±20.5
KQK5	41°41'29"	80°06'52"	3327	7.8	1.59	13.5	3.59	0.1237	3.2	2061.2	440.6±41.7

outwash sand samples from the bottom of the natural profile close to the snout of the Keqicarbaxi glacier had OSL and ESR ages of 7.3 ± 0.8 ka (Kqk-29[#]) and 6.8 ± 0.6 ka (Kqk-1), respectively. The tills underlying the outwash sand were deposited in during the early Holocene, and might be associated with the 8.2 ka cooling event.

The ESR ages for the second set of moraines were: 14.3 ± 1.3 ka (No. 6), 18.1 ± 1.8 ka (No. 9), 21.1 ± 2.1 ka (Kqk-3), 17.4 ± 1.6 ka (Kqk-5) and 26.7 ± 2.5 ka (No. 19) and show that the moraines formed during MIS 2. Four ages are the same statistically, only one (No. 19) is statistically older. Our field mapping shows that the Keqicarbaxi glacier was ~29 km long during this time. Two ESR samples from the first set of moraines on the Kekewulongsu River, ~3 km west of the Qingshantou glacial plateau, have ages of 20.5 ± 1.9 ka (No. 2) and 26.8 ± 2.5 ka (No. 11). These overlap with the five ages of the second set from the Ateaoyinake River. Together, the ESR ages suggest that one or maybe two advances occurred during MIS 2, at about 18–21 ka and 28 ka.

We also measured an OSL age, 12.3 ± 1.2 ka (Kqk-19[#]), for the innermost end moraine of this set. This age is consistent with the Younger Dryas Stade, therefore, the formation time of this moraine should be taken in assigning to this Stade on the basis of a single age.

In recent years, studies undertaken on the south slope of Himalayas indicated that the extent of glaciation there during MIS 3 was greater than that during the LGM_C (Owen et al., 2002a,b,c; Zech et al., 2003; Kamp et al., 2004). These studies suggest that advances of these glaciers likely relate to the time of enhanced Indian-monsoon circulation, when increased summer precipitation results in positive mass balance and allows the glaciers to advance.

The $\delta^{18}\text{O}$ record in the Guliya ice core shows that multiple cold events occurred during MIS 3 (Thompson et al., 1997; Yao et al., 1997). During these events, the temperature in northwestern Tibet was as low as in MIS 2 and 4. Shi and Yao (2002) subdivided MIS 3 into three sub-stages (a, b and c) based on the same isotopic record and other considerations (e.g., precessional cycle). The MIS 3b (44–54 ka) was wet as well as cold. Evidence from geomorphic and sedimentological data show that high lake levels also occurred in the Qinghai–Tibetan Plateau and in the northwestern area of China in the middle and late

part of MIS 3 (e.g., Jia et al., 2001; Shi et al., 2002; Zhang et al., 2004), thus indicating high precipitation during that time that likely caused glaciers to advance.

The third set of moraines date to 40.9 ± 4.0 ka (Kqk-4), 46.2 ± 4.2 ka (No. 18), 51.0 ± 4.8 ka (No. 13) and 54.0 ± 5.2 ka (No. 16). Given the analytic precision, these ages possibly demonstrate that this set of moraines related to a MIS3b glacial advance. The extent of this glacial advance is about the same as that of the LGM_C. This also suggests that abundant precipitation occurred during this time.

Three ESR dates of the fourth set of moraines and outwash are 62.3 ± 5.8 ka (No. 5), 55.4 ± 5.2 ka (No. 8, outwash) and 60.2 ± 5.7 ka (No. 4, outwash). The age for the well-sorted fluvial gravel that unconformably lies beneath the drift is 122.3 ± 11.7 ka (No. 17) (Fig. 9). These results indicate that the moraines and the outwash are from the early period of Last Glacial, during MIS 4. The Keqicarbaxi glacier was ~35 km long at this time.

Two dates were obtained from the fifth set of moraines: 134.4 ± 12.6 ka (No. 14) and 219.7 ± 20.5 ka (No. 15). The dates do not overlap and might not represent the same event, but they bracket the three published ESR ages (171.1 ± 17 , 176 ± 18 , and 184.7 ± 18 ka) from the lower part of the Xiawangfeng till near the house of the Wangfeng road maintenance squad on the Ürümqi River in the eastern Tianshan Mountains (Zhao et al., 2006). They date to MIS 6, and indicate that the Keqicarbaxi glacier had expanded onto the piedmont during the penultimate glacial. The glaciers were more than 10 km wide and about 37 km long at this time.

A single sample from the Qingshantou till dates to 440.6 ± 41.7 ka (KQK5) and likely represents a glacial advance during MIS 12. This is consistent with ESR ages (459.7 ± 46 and 471.1 ka) from an old deposit, mapped as the "Gaowangfeng till," above the Ürümqi River (Zhou et al., 2001; Zhao et al., 2006). These ages suggest that the central and eastern segments of the Tianshan Mountains were sufficiently elevated to develop glaciers during the mid-Pleistocene.

The ESR chronology in this study and the published geochronology near the headwaters of the Ürümqi River (Zhao et al., 2006) indicate that the glaciations in the central and eastern parts of the Tianshan

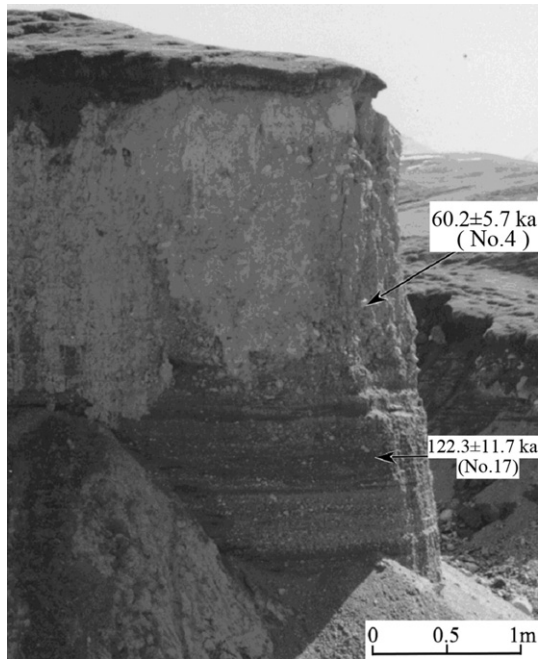


Fig. 9. Section of outwash and the underlying well-sorted fluvial deposits (41°43'35"N, 80°11'41"E).

Mountains are synchronous. Developing a chronology of the glacial landforms in this area is the first step towards understanding glacial and landscape evolution in this region.

7. Conclusion

The Ateoyinake River Valley in the Tianshan Mountains has experienced multiple glaciations. These occurred during the late Holocene, MIS 2, MIS 3b, MIS 4, MIS 6, and MIS 12. During the late Holocene the Keqicarbaxi glaciers advanced about 27 km.

Large compound valley glaciers occurred in MIS 2–3, while wide terminal valley glaciers formed in MIS 4, and piedmont glaciers in MIS 6. The lengths were 31 km, 35 km, and 37 km, respectively. The oldest glaciation, during MIS 12 (Qingshantou Glacial Stage), correlates with the Gaowangfeng till of the Ürümqi River. This chronology provides a framework and first step towards defining rates of landscape evolution in the glaciated regions of the Tianshan Mountains.

Acknowledgements

We thank Dr Shanguan Donghui and Dr Wang Jie for their fieldwork assistance. Diao Shaobo for helping to analyze the ESR samples in the Open Laboratory of Marine Sedimentology, Qingdao. Alan R Gillespie and Karen Gillespie for their helpful comments and suggestions to help us to improve our manuscript, scientific editors Lewis A Owen and Yi Chaolu and two anonymous reviewers for their helpful comments and suggestions. This research was supported by the National Natural Science Foundation of China (Grant Nos. 40501007, 40571034, 90511007), West Light Foundation of the CAS (2005YU04), National Basic Research Program of China (No. 2007CB411500) and the Knowledge Innovation Project of CAS (Grant No. KZCX2-YW-301 and KZCX3-SW-345).

References

Adamiec, G., Aitken, M.J., 1998. Dose-rate conversion factors: update. *Ancient TL* 16, 37–50.

Brocklehurst, S.H., Whipple, K.X., 2006. Assessing the relative efficiency of fluvial and glacial erosion through simulation of fluvial landscapes. *Geomorphology* 75, 283–299.

Buhay, W.M., Schwarcz, H.P., Grün, R., 1988. ESR dating of fault gouge: the effect of grain size. *Quaternary Science Reviews* 7, 515–522.

Feidaoluweiqi, B.A., Yan, Q.S., 1959. New data of the times and features about the Tianshan Mountains' ice ages in China. *Memoirs of the natural conditions in Xinjiang Province (memoirs)*. Science Press, Beijing, pp. 14–31 (in Chinese).

Feidaoluweiqi, B.A., Yan, Q.S., 1960. Study on the times and features of the Tianshan Mountains' ice ages in the western China. *Quaternary Sciences in China* 3 (1–2), 9–33 (in Chinese).

Finkel, R.C., Owen, L.A., Barnard, P.L., Caffee, M.W., 2003. Beryllium-10 dating of Mount Everest moraines indicates a strong monsoonal influence and glacial synchronicity throughout the Himalaya. *Geology* 31, 561–564.

Geography Department of Nanjing University (Geomorphology teaching and research section), 1974. *Quaternary glaciations and ice ages in China*. Science Press, Beijing, pp. 1–9, 28–30, 125–142 (in Chinese).

Gillespie, A.R., Molnar, P., 1995. Asynchronism of maximum advances of mountain and continental glaciations. *Reviews of Geophysics* 33, 311–364.

Hallet, B., Hunter, L., Bogen, J., 1996. Rates of erosion and sediment evacuation by glaciers: a review of field data and their implications. *Global and Planetary Change* 12, 213–235.

Huang, T.K., 1944. Pleistocene morainic and non-morainic deposits in the Taglag area, north of Agsu, Sinkiang. *Bulletin of Geological Society of China* 24 (1–2), 125–145.

Jia, Y.L., Shi, Y.F., Wang, S.M., Jiang, X.Z., Li, S.J., Wang, Ai-J., Li, X.S., 2001. Lake expanding events in the Tibetan Plateau since 40 ka BP. *Science in China (Ser. D)* 44, 301–315 (suppl.).

Kamp Jr., U., Haserodt, K., Shroder Jr., J.F., 2004. Quaternary landscape evolution in the eastern Hindu Kush, Pakistan. *Geomorphology* 57, 1–27.

Lanzhou Institute of Glaciology and Geocryology, CAS (Ed.), 1985. *Glacier Inventory of China III: Tianshan Mountains (Interior Drainage Area of Tarim Basin in Southwest)*. Science Press, Beijing, p. 69 (in Chinese).

Liu, Z.C., Liu, Z.Z., Wang, F.B., 1962. A comparison of the Quaternary glaciers development patterns nearby the Qomolangma Peak, Hantengri Peak and the Tuanjie Peak of Qilianshan Mountains. *Acta Geographica Sinica* 28 (1), 21–33 (in Chinese with Russian abstract).

Mahaney, W.C., Vortisch, W., Julig, P.J., 1988. Relative differences between glacially crushed quartz transported by mountain and continental ice: some examples from North America and East Africa. *American Journal of Science* 288, 810–826.

Molnar, P., England, P., 1990. Late Cenozoic uplift of mountain ranges and global climate change: chicken or egg? *Nature* 346, 29–34.

Murray, A.S., Wintle, A.G., 2000. Luminescence dating of quartz using an improved single-aliquot regenerative-dose protocol. *Radiation Measurements* 32, 57–73.

Owen, L.A., Finkel, R.C., Caffee, M.W., 2002a. A note on the extent of glaciation throughout the Himalaya during the global Last Glacial Maximum. *Quaternary Science Reviews* 21, 147–157.

Owen, L.A., Kamp, J., Spencer, J.Q., Haserodt, K., 2002b. Timing and style of Late Quaternary glaciation in the eastern Hindu Kush, Chitral, northern Pakistan: a review and revision of the glacial chronology based on new optically stimulated luminescence dating. *Quaternary International* 97/98, 41–55.

Owen, L.A., Finkel, R.C., Caffee, M.W., Gualtlen, L., 2002c. Timing of multiple late Quaternary glaciations in the Hunza Valley, Karakoram Mountains, northern Pakistan: defined by cosmogenic radionuclide dating of moraines. *Geological Society of America Bulletin* 114 (5), 593–604.

Owen, L.A., Finkel, R.C., Ma, H.Z., Spencer, J.Q., Derbyshire, E., Barnard, P.L., Caffee, M.W., 2003. Timing and style of late Quaternary glaciation in northeastern Tibet. *Geological Society of America Bulletin* 115 (11), 1356–1364.

Owen, L.A., Caffee, M., Bovard, K., Finkel, R.C., Sharma, M.C., 2006a. Terrestrial cosmogenic nuclide surface exposure dating of the oldest glacial successions in the Himalayan orogen: Ladakh Range, Northern India. *Geological Society of America Bulletin* 118 (3–4), 383–392.

Owen, L.A., Finkel, R.C., Ma, H.Z., Barnard, P.L., 2006b. Late Quaternary landscape evolution in the Kunlun Mountains and Qaidam Basin, Northern Tibet: a framework for examining the links between glaciation, lake level changes and alluvial fan formation. *Quaternary International* 154/155, 73–86.

Prescott, J.R., Hutton, J.T., 1994. Cosmic ray contributions to dose rates for luminescence and ESR dating: large depths and long-term time variations. *Radiation Measurements* 23 (2–3), 497–500.

Raymo, M.E., Ruddiman, W.F., 1992. Tectonic forcing of late Cenozoic climate. *Nature* 359, 117–122.

Shi, Y.F., Yao, T.D., 2002. MIS 3b (54–44 ka BP) cold period and glacial advance in middle and low latitudes. *Journal of Glaciology and Geocryology* 21 (1), 1–9 (in Chinese with English Abstract).

Shi, Y.F., Zheng, B.X., Su, Z., Mu, Y.Z., 1984. Study of Quaternary glaciation in Mts. Tomui-hantengri area, Tianshan. *Journal of Glaciology and Cryopedology* 6 (2), 1–14 (in Chinese with English Abstract).

Shi, Y.F., Zheng, B.X., Su, Z., 2000. Glaciations, glacial-interglacial cycles and environmental changes in the Quaternary. In: Shi, Y.F. (Ed.), *Glaciers and their Environments in China—the Present, Past and Future*. Science Press, Beijing, pp. 320–355 (in Chinese).

Shi, Y.F., Jia, Y.L., Yu, G., Yang, D.Y., Fan, Y.Q., Li, S.J., Wang, Y.F., 2002. Features, impacts and causes of the high temperature and large precipitation event in the Tibetan Plateau and its adjacent area during 40–30 ka BP. *Journal of Lake Sciences* 14 (1), 1–11 (in Chinese with English abstract).

Spencer, J.Q., Owen, L.A., 2004. Optically stimulated luminescence dating of Late Quaternary glaciogenic sediments in the upper Hunza valley: validating the timing of glaciation and assessing dating methods. *Quaternary Science Reviews* 23, 175–191.

Su, Z., Zheng, B.X., Shi, Y.F., Wang, Z.C., 1985. Quaternary glacial remains and the determination of glacial period in Mt. Tumor district. In: *Scientific Expedition Team on Mountaineering of the Chinese Academy of Sciences (Ed.), Glacier and Meteorology in Tumor Peak Region, Tianshan Mountains*. Xinjiang People's Publishing House, Urumqi, pp. 1–31 (in Chinese).

- Tanaka, T., Sawada, S., Ito, T., 1985. ESR dating of late Pleistocene near-shore and terrace sands in southern Kanto, Japan. In: Ikeya, M., Miki, T. (Eds.), *ESR Dating and Dosimetry*. Ionics, pp. 275–280. Tokyo.
- Thompson, L.G., Yao, T., Davis, M.E., Henderson, K.A., Thompson, E.M., Lin, P.N., Beer, J., Synal, H.A., Cole-Dai, J., Bolzan, J.F., 1997. Tropical climate instability: the last glacial cycle from a Qinghai–Tibetan ice core. *Science* 276, 1821–1825.
- Walther, R., Zilles, D., 1994. ESR studies on bleached sedimentary quartz. *Quaternary Science Reviews* 13 (5–7), 611–614.
- Yao, T.D., Thompson, L.G., Shi, Y.F., Qin, D.H., Jiao, K.Q., Yang, Z.H., Tian, L.D., Thompson, E.M., 1997. Climate variation since the Last Interglaciation recorded in the Guliya ice core. *Science in China (Ser. D)* 40 (6), 662–668.
- Ye, Y.G., He, J., Diao, S.B., Gao, J.C., 1993. ESR dating of the coastal wind sand of late Pleistocene. *Marine Geology & Quaternary Geology* 13 (3), 85–89 (in Chinese).
- Ye, Y.G., Diao, S.B., He, J., Gao, J.C., Lei, X.Y., 1998. ESR dating studies of Paleo-debris-flows deposition Dongchuan, Yunnan province, China. *Quaternary Science Reviews (Quaternary Geochronology)* 17, 1073–1076.
- Yi, C.L., 1997. Subglacial comminution—evidence from microfabric studies and grain size analysis. *Journal of Glaciology* 43, 174–179.
- Yi, C.L., Li, X.Z., Qu, J.J., 2002. Quaternary glaciation of Puruogangri—the largest modern ice field in Tibet. *Quaternary International* 97/98, 111–121.
- Zech, W., Glaser, B., Abramowski, U., Dittmar, C., Kubik, P.W., 2003. Reconstruction of the Late Quaternary Glaciation of the Macha Khola valley (Gorkha Himal, Nepal) using relative and absolute (^{14}C , ^{10}Be , dendrochronology) dating techniques. *Quaternary Science Reviews* 22, 2253–2265.
- Zhang, H.C., Peng, J.L., Ma, Y.Z., Chen, G.J., Feng, Z.D., Li, B., Fan, H.F., Chang, F.Q., Lei, G.L., Wünnemann, B., 2004. Late Quaternary palaeolake levels in Tengger Desert, NW China. *Palaeogeography, Palaeoclimatology, Palaeoecology* 211, 45–58.
- Zhang, W., Cui, Z.J., Feng, J.L., Yi, C.L., Yang, J.Q., 2005. Late Pleistocene glaciation of the Hulifang massif of Gongwang Mountains in Yunnan Province. *Journal of Geographical Sciences* 4, 448–458.
- Zhao, J.D., Zhou, S.Z., He, Y.Q., Ye, Y.G., Liu, S.Y., 2006. ESR dating of glacial tills and glaciations in the Urumqi River headwaters, Tianshan Mountains, China. *Quaternary International* 144, 61–67.
- Zheng, B.X., 1985. Glacial geomorphological map (1:200000) of Mt. Tomur region, Tianshan. *Annals of Glaciology* 8, 209.
- Zhou, S.Z., Li, J.J., 1998. The sequence of Quaternary glaciation in the Bayan Har Mountains. *Quaternary International* 45/46, 135–142.
- Zhou, S.Z., Yi, C.L., Shi, Y.F., Ye, Y.G., 2001. Study on the ice age MIS 12 in Western China. *Journal of Geomechanics* 7 (4), 321–327 (in Chinese with English Abstract).
- Zhou, S.Z., Jiao, K.Q., Zhao, J.D., Zhang, S.Q., Cui, J.X., Xu, L.B., 2002a. Geomorphology of the Urumqi River Valley and the uplift of the Tianshan Mountains in Quaternary. *Science in China (Ser. D)* 45 (11), 961–968.
- Zhou, S.Z., Li, J.J., Zhang, S.Q., 2002b. Quaternary glaciation of the Bailang River Valley, Qilian Shan. *Quaternary International* 97/98, 103–110.
- Zhou, S.Z., Wang, X.L., Wang, J., Xu, L.B., 2006. A preliminary study on timing of the oldest Pleistocene glaciation in Qinghai–Tibetan Plateau. *Quaternary International* 154/155, 44–51.